

*Refereed Proceedings*

*The 12th International Conference on  
Fluidization - New Horizons in Fluidization  
Engineering*

---

Engineering Conferences International

Year 2007

---

An Analysis of Pressure Fluctuations in a  
CFB of Heavy Minerals

Adam Luckos\*

Quinn G. Reynolds †

Paul den Hoed‡

\*Sasol Technology, South Africa, [adam.luckos@sasol.com](mailto:adam.luckos@sasol.com)

†Mintek, South Africa, [quinnr@mintek.co.za](mailto:quinnr@mintek.co.za)

‡Mintek, South Africa, [denhoed@mintek.co.za](mailto:denhoed@mintek.co.za)

This paper is posted at ECI Digital Archives.

[http://dc.engconfintl.org/fluidization\\_xii/16](http://dc.engconfintl.org/fluidization_xii/16)

## AN ANALYSIS OF PRESSURE FLUCTUATIONS IN A CFB OF HEAVY MINERALS

A. Luckos,<sup>†</sup> Q.G. Reynolds and P. den Hoed

MINTEK, Private Bag X3015, Randburg 2125, South Africa

<sup>†</sup>Now with Sasol Technology, P.O. Box 1, Sasolburg 1947, South Africa

### ABSTRACT

Pressure fluctuations were measured at high frequencies in a CFB model operated with air at ambient conditions. The model comprises an 80-mm-ID, 5-m-tall riser with a blind-T exit, a cyclone, a 50-mm-ID standpipe, and an L-valve. Tests were conducted with particles of natural rutile ( $\text{TiO}_2$ ), a heavy mineral mined from coastal dunes. The particles fall into group B of Geldart's classification. The solids inventory was kept at 25 kg. The superficial gas velocity ranged from 3 to 6 m/s. The solid circulation flux varied between 10 and 40  $\text{kg/m}^2\cdot\text{s}$ .

Profiles of solid concentrations in the riser are C-shaped. The amplitude of pressure fluctuations increases with increasing solids-circulation rate, and the increase appears to be linear. The amplitude does not correlate with solids concentration, however. The implication is that gas-solid interactions differ significantly at the bottom and the top of the riser, despite similar solids concentrations in these two zones. The analysis in the frequency domain shows that the power of signals resides in those of low frequencies (<2 Hz). The pressure fluctuations reflect white noise: there is no dominant frequency and no periodic component. Pressure waves move at 25–45 m/s up the riser, an order of magnitude greater than the superficial gas velocity.

### INTRODUCTION

Two heavy minerals, ilmenite (nominally  $\text{FeTiO}_3$ ) and rutile ( $\text{TiO}_2$ ), and their derivatives, titaniferous slag (86% " $\text{TiO}_2$ "), upgraded slag (95%  $\text{TiO}_2$ ) and synthetic rutile (95%  $\text{TiO}_2$ ), are raw materials in the production of titania pigment and titanium metal. In the chloride process, chlorination in a bubbling fluidized bed is central to the production of these commodities. The case has been argued that, for southern Africa—which produces comparatively little titania pigment, none of it by the chloride process, yet provides a quarter of the world's titanium-bearing feedstock—a circulating fluidized bed may have economic and technical advantages over a bubbling bed, the standard in the industry (1). It was to test this potential that Mintek built a pilot plant, a 5-m-tall CFB reactor of graphite, and a cold (PVC) model of identical dimensions. Tests in the cold model (in which process variables could be measured) have revealed a great deal about the workings of the high-temperature reactor. Such fundamental variables as  $U_{mf}$  and  $U_t$  were determined in the cold model (2). Recent tests have measured the distribution of solid (heavy-mineral) concentrations in the riser (3–4). Pressure fluctuations, the subject of this paper, have now been measured. By their analysis we hope to assess the quality of fluidization of heavy minerals in the CFB. In time, as more conditions are tested and data collected, so our analysis should establish the relationships between three entities, (1) process variables, (2) the physical properties of heavy minerals, and (3) pressure

fluctuations at different levels in the riser. These relationships will provide a basis for controlling the operation of a CFB chlorinator of heavy minerals.

## TEST PROCEDURE

The riser of the CFB cold model, which divides into five sections of transparent PVC, stands 5 m tall; its internal diameter is 80 mm. The distributor is a perforated plate (2-mm holes covering ~5% of the plate) covered by a 106- $\mu\text{m}$  mesh. The exit is a blind T; the blank flange at the top of the column sits 85 mm above the top of the exit to the cyclone. Taps are located at intervals along the column on the side opposite the inlet and exit. Each one provides an opening for a pressure transducer to measure the pressure at the wall in the column. Data acquisition units record the signals from these transducers. Another three pressure transducers with faster response times (1 ms) span the column, at the bottom (0.2 m above the distributor), in the middle (at 2.46 m), and at the top of the riser (at 4.47 m). These transducers were calibrated to measure pressures from zero to 14 kPa. The apparatus is described in an earlier paper on the subject (3).

Measurements were conducted for different solid-circulation rates at three fluidizing velocities—8 conditions in all. Gauge pressures at the side-wall were sampled at a frequency of 200 Hz. At each stable condition signals were collected over a period 40 s, an interval producing 8192 (i.e.,  $2^{13}$ ) pressure readings. Pressures were also measured at less frequent intervals at the other taps on the riser. The solid material under circulation was natural rutile ( $\text{TiO}_2$ ) from a beach-sand deposit on the west coast of South Africa. Its particles fall into Group B of Geldart's classification. They are sub-rounded, fine (80–165  $\mu\text{m}$ ) and dense (4085  $\text{kg/m}^3$ ) (2).

## RESULTS

The pattern of observations repeats the pattern of earlier studies (3–4). The concentration of solids in the riser adopts a C shape, which becomes less pronounced as the solids-circulation rate,  $G_s$ , at a given fluidizing velocity,  $U$ , decreases (see Figure 1a). Concomitant with the decrease is a shift in solids concentration at each point in the column to lower values, and a move to greater solids concentrations at the top of the column than at the bottom. A higher suspension density at the top of the column—a consequence of the rebounding of particles from the plate closing the top of the riser, an abrupt exit—is a phenomenon that is well documented and studied in small-scale (<0.2 m) CFB units (5–8). In tests with rutile at a comparatively low fluidizing velocity (3.5 m/s), higher solids concentrations span the top half of the riser (~2.5 m). The suspension density decreases gradually from the top of the column. At higher fluidizing velocities ( $U = 4.9$  and  $7.4$  m/s) higher solids concentrations are confined to a shorter length of the riser ( $\leq 1$  m), and the profile is much steeper (see 3). As Jin and co-workers showed, higher superficial gas velocities increase the velocity of upwardly moving particles, which increases the exchange of momentum between particles moving in opposite directions (9). As the influence of upwardly moving particles grows stronger (at high gas velocities), the region of momentum exchange shortens. A shortening of the region of higher suspension densities would accompany this change.

Pressures in the column fluctuate over a range of about 1.2 kPa; the patterns of fluctuations along the length of the column are similar and synchronized (see Figure 1b, which is typical of pressure fluctuations measured for all conditions). Pressure fluctuations are irregular, and peak intensities vary. The distribution of pressures at each tap is skewed towards higher values: fluctuations are more pronounced above the mean than below it (see Figure 1). Expressing the amplitude of fluctuations over a scanned interval by the standard deviation of pressure readings, one can readily see that—

- The average amplitude of pressure fluctuations increases with increasing  $G_s$  and  $U$ .

- The average amplitude of fluctuations is largest at the top of the column; the amplitudes of fluctuations at the middle and bottom of the column are similar—yet the solids concentration is similar at the top and bottom, and different from that in the middle.
- There is an exception to this pattern at high superficial gas velocities. The measurements may be problematic as solids flow bordered on being unstable.

Pressure increases with increasing superficial gas velocity and solids-circulation rate. Over the range of conditions tested (which we acknowledge to be narrow) there appears to be a linear relationship between the standard deviation of pressure readings (a measure of the amplitude of pressure fluctuations) and the solids-circulation rate,  $G_s$  (see Figure 2).

Two test conditions produced pneumatic transport, the mode of transport in which solids move up the column in a very lean phase; reflux is reduced and the solids-concentration profile is “flat” (cf. Figure 1a).

### Frequency-domain analysis

Information about the hydrodynamics of gas-solid flow in a CFB can be gleaned from an analysis of pressure signals in the frequency domain (10–12). In particular, the power spectral density and its inverse Fourier transform, the autocorrelation function—which measures time delays between similar events in the column—can identify periodic components, if any, in pressure fluctuations. From the cross-correlation between, say, taps at the bottom and top of the column one can determine the average velocity of pressure waves propagating up the riser.

The mathematics underlying this analysis is well-documented (10–11, 13). Our time-sample data are the pressure measurements and their associated times (see Figure 1b). These data form the series  $f_k$ , with  $N$  samples taken at sampling period  $\Delta t$ . The discrete Fourier-transform series,  $F_n$ , is calculated from this series. The power spectrum series,  $P_n$ , is the square of the complex modulus of the Fourier transform, and the autocorrelation function series,  $a_k$ , is the inverse discrete Fourier transform of the power spectral density. The cross-correlation,  $c_{12,k}$ , between data sets is also computed through Fourier transforms. Each data set is transformed by the FFT algorithm. The result of the first is then multiplied by the complex conjugate of the second. The product is transformed by the inverse FFT to give the cross-correlation series (13).

Figure 3a shows the spectral power densities of the pressure signals in condition 2 of test 2 ( $U = 4.17$  m/s and  $G_s = 21.8$  kg/m<sup>2</sup>·s—see Figure 1b). Fifty-five to sixty per cent of total power sits in frequencies less than 1 Hz; another 25–30% of power sits in frequencies 1–2 Hz. Seven major frequencies between them account for 25% of the total energy. Of significance, however, is the absence of any concentration of power in a narrow band of frequencies—the power spectral density lacks a dominant frequency. There is, in other words, no periodic component to pressure fluctuations in the riser. This condition is also indicated in the autocorrelation function, which decays rapidly as time lag increases (Figure 3b): the pressure fluctuations are those of white noise. The absence of periodicity in the pressure fluctuations in CFBs (but not in bubbling fluidized beds) was noted by Johnsson and co-workers (10).

Changes in the power spectral density show how conditions affect pressure fluctuations in the CFB. For a given fluidizing velocity, as  $G_s$  increases, the total power in the signal increases and more power sits in frequencies below the strongest one (the highest peak—see Figure 3a); and the strongest frequency shifts to lower values. We see, for example, that—

At  $U = 3.57$  m/s, increasing  $G_s$  from 14.8 kg/m<sup>2</sup>·s to 19.2 kg/m<sup>2</sup>·s shifts the strongest

frequency from 1.29 Hz to 1.17 Hz.

- At  $U = 4.17$  m/s, increasing  $G_s$  from  $17.8$  kg/m<sup>2</sup>·s to  $21.8$  kg/m<sup>2</sup>·s shifts the strongest frequency from 0.95 Hz to 0.83 Hz

Increasing  $U$  has a similar effect: at a given  $G_s$  increasing  $U$  shifts the strongest frequency to lower values.

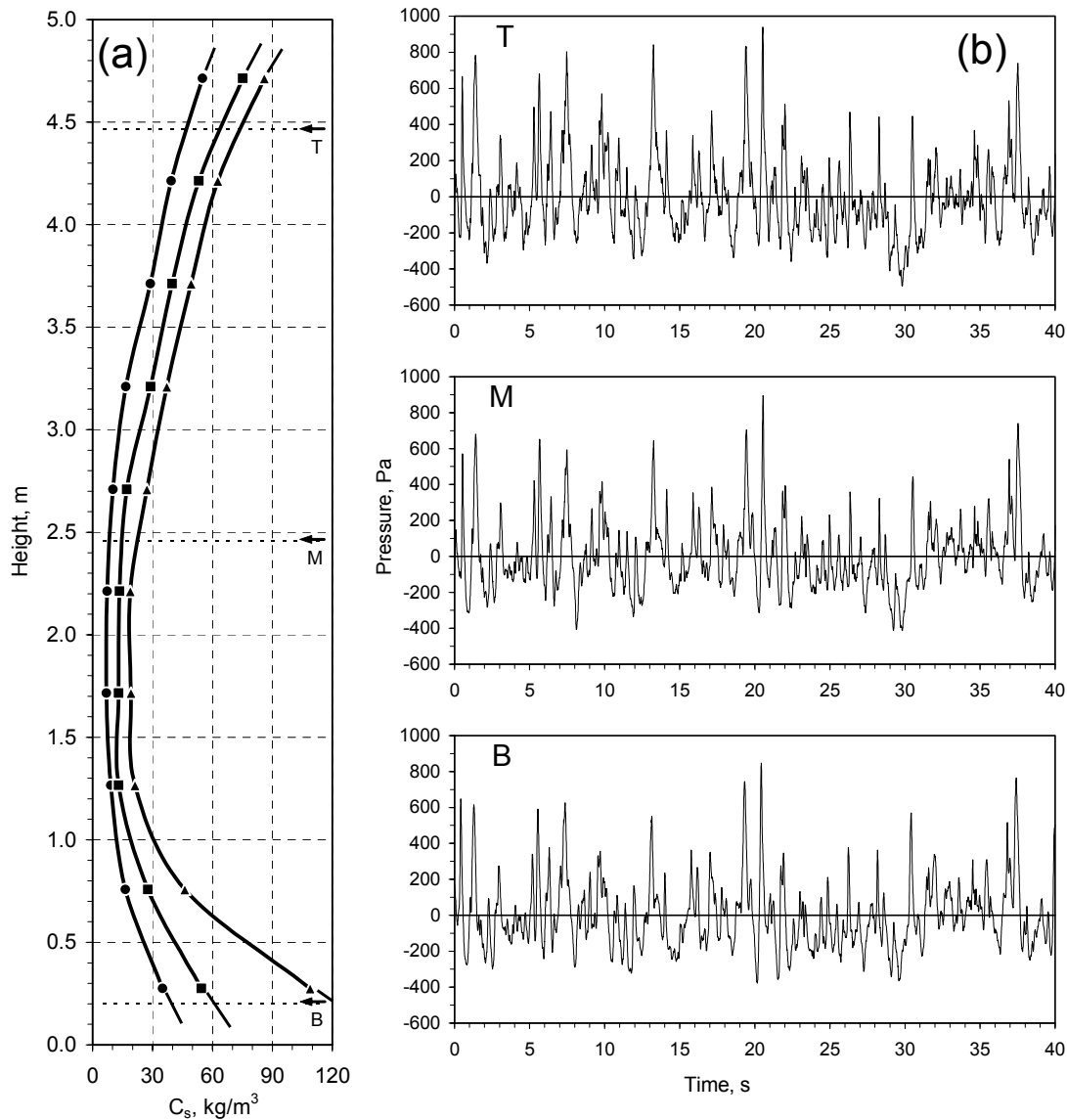


Figure 1. Solids concentrations and pressure fluctuations at points along the riser.

(a) Solids concentrations at  $U = 3.5$  m/s and  $G_s = 17.8$  kg/m<sup>2</sup>·s (●),  $21.8$  kg/m<sup>2</sup>·s (■), and  $26.8$  kg/m<sup>2</sup>·s (▲)

(b) Pressure fluctuations: the 0-Pa line in each graph marks the average for the readings captured ( $U = 4.17$  m/s and  $G_s = 21.8$  kg/m<sup>2</sup>·s)

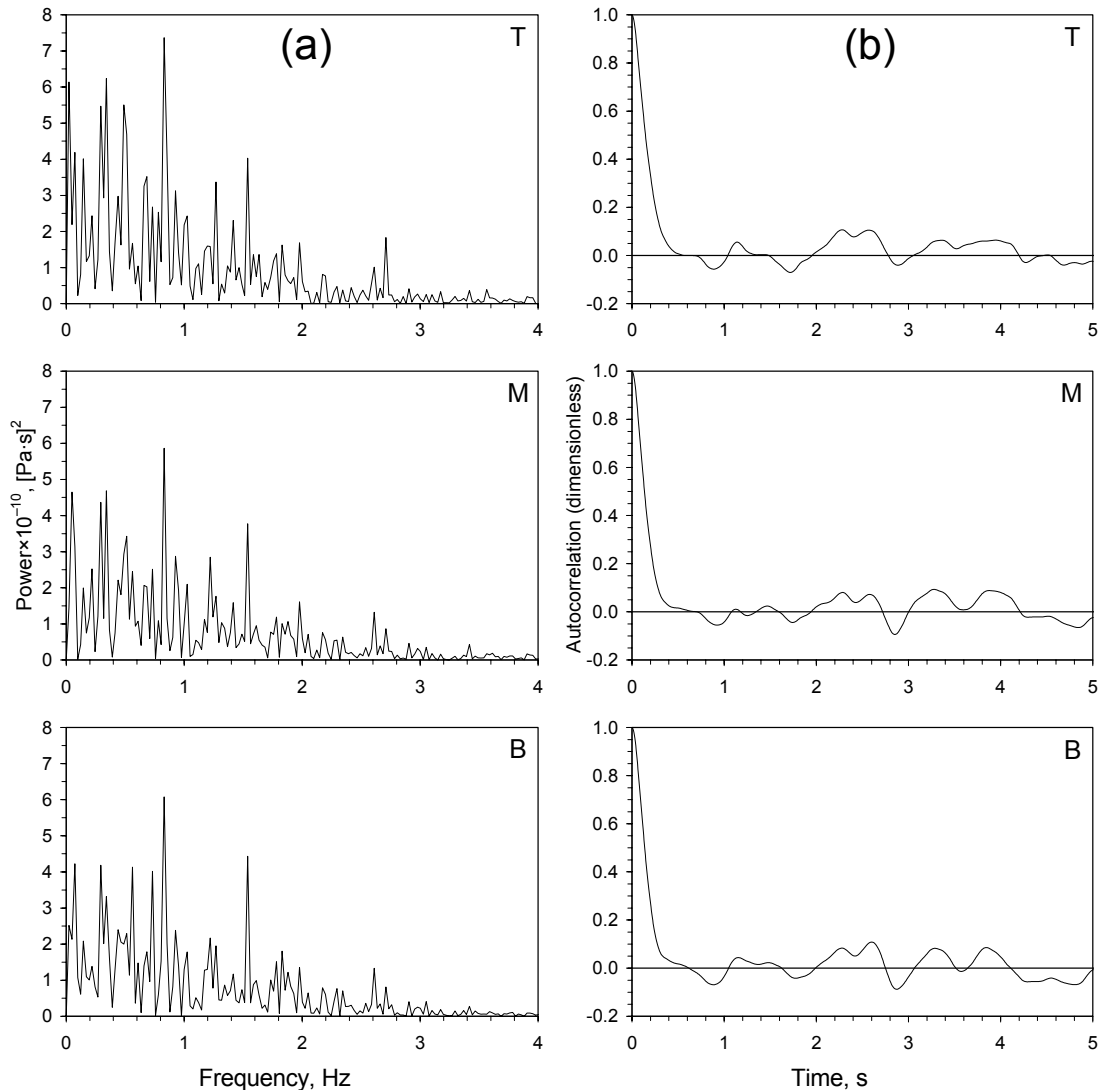
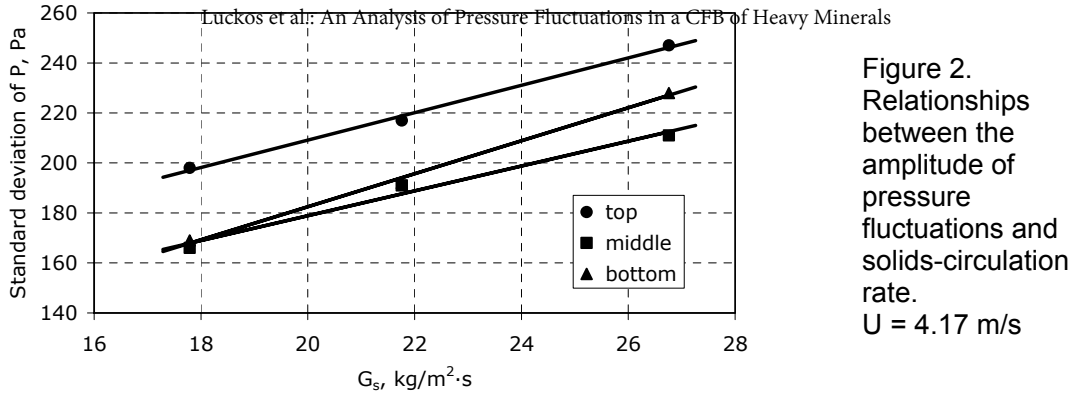


Figure 3. Analysis of pressure fluctuations in the frequency and time domains ( $U = 4.17 \text{ m/s}$  and  $G_s = 21.8 \text{ kg/m}^2\cdot\text{s}$ ): (a) Power spectral densities at the top (T), middle (M) and bottom (B) of the riser; (b) Autocorrelation of pressure signals at the top, middle and bottom of the riser (signals depicted in figure 1b) The pressure waves of noise are propagated up the riser. The upward direction is indicated

by the short delay in corresponding forms of pressure signals at the bottom, middle and top of the riser (Figure 1b). Cross-correlations of signals from the bottom and top of the riser show that an increase in pressure at the top of the column followed an increase at the bottom of the column by a tenth to a fifth of a second (Figure 4). Depending on conditions (solids-circulation rate and fluidizing velocity), pressure waves travel at between 25 and 45 m/s (Table 1). Propagation velocities are an order of magnitude greater than the superficial gas velocities and an order of magnitude smaller than the velocity of sound in air (344 m/s).

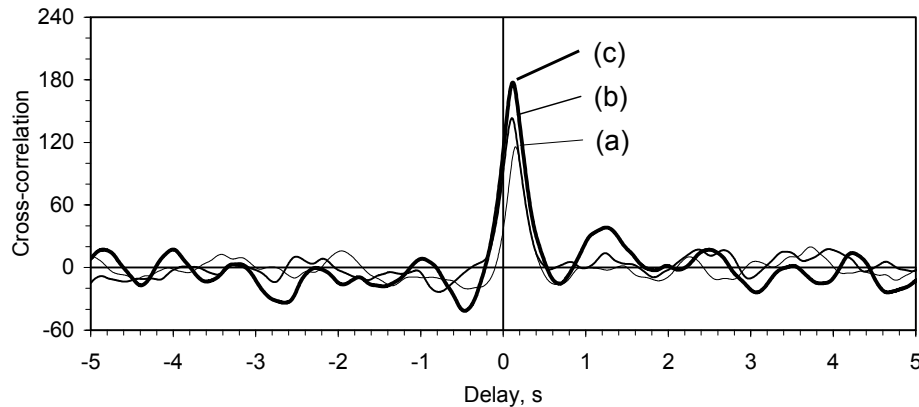


Figure 4. Cross-correlations of pressure fluctuations between top and bottom of riser for test 2 ( $U = 4.17$  m/s): (a)  $G_s = 17.8$  kg/m<sup>2</sup>·s, (b)  $G_s = 21.8$  kg/m<sup>2</sup>·s, and (c)  $G_s = 26.8$  kg/m<sup>2</sup>·s.

Table 1. Summary of set and measured variables

$G_s$ , kg/m <sup>2</sup> ·s	Average solids concentration, $C_s$ , kg/m <sup>3</sup>	Speed of pressure waves, m/s	Intensity of cross-correlation peak
<b>Test 1, <math>U = 3.57</math> m/s</b>			
11.5 <sup>†</sup>	15.9	26	27
14.8	27.4	41	67
19.2	43.7	27	82
<b>Test 2, <math>U = 4.17</math> m/s</b>			
17.8	22.1	28	116
21.8	33.1	41	143
26.8	46.2	37	177
<b>Test 3, <math>U = 4.78</math> m/s</b>			
29.7 <sup>†</sup>	10.2	45	123
34.2 <sup>‡</sup>	31.9	21	207

<sup>†</sup> The CFB ran in the pneumatic mode of fluidization

<sup>‡</sup> The flow of solids through the L-valve was unstable

## CONCLUDING REMARKS

Arriving at an understanding of the hydrodynamics of fluidized beds by an analysis of pressure fluctuations is an approach explored by many researchers. Far fewer are applications of the approach to the study of phenomena in circulating fluidized beds (12, 14–21). Although group-b particles are generally treated, the materials are all light (silica sand). Our study is the first to explore the hydrodynamics of a circulating fluidized bed of rutile, a

heavy mineral, which is defined as one with an  $sg$  greater than 2.9. In many respects the hydrodynamics of a fine heavy mineral in a cfb are qualitatively similar to those of coarser silica sand ( $sg$  2.6). One finds that the power spectral density, for example, is concentrated in frequencies of 10 hz and lower, if not 4 hz and lower (18, 14). Not surprisingly, too, solids are concentrated more heavily at the bottom of the riser; and increasing the superficial gas velocity raises pressures and lowers local solids concentrations (20). But, as these studies were conducted in cfbs with smooth exits, there is—unlike in our study—no increase in solids concentration at the top of the riser. There does appear to be a difference, however, in the direction of change in the average amplitude of fluctuations with changes in certain process variables. In at least two studies of fluidized beds of silica sand or fcc in dilute flow, the average amplitude of pressure fluctuations decreased with increasing superficial velocity or increasing solids hold-up (14–15). Our measurements showed pressure fluctuations becoming more extreme with increasing  $u$  or  $c_s$  (see figure 2, table 1).

The conclusions drawn from the observations reported in this paper are tentative. More data are needed to confirm the relationships. The linear change in the amplitude of fluctuations with  $G_s$ , the solids-circulation rate, for example, is suggested by only three points on a line. Should this relationship be confirmed, we should have a measure of, and hence the means to control,  $G_s$ . We also need to assess whether core-annulus flow produces marked differences between pressures at the wall (which the pressure transducers measure) and pressures along the axis of the column.

That the fluctuations in pressure show no periodicity—that they are noise—is of more academic interest. Such signals are a product of fast fluidization, the regime in which one would want to run a CFB.

## ACKNOWLEDGMENTS

Our thanks go to the (South African) Department of Science and Technology, through the Innovation Fund, for a grant (project No. 32211) that made possible the construction of the CFB cold model; and to our colleague Dr Ian Barker for discussions on the interpretation of the results of Fourier analyses.

## REFERENCES

1. Den Hoed, P. Freeman, M.J., Luckos, A. and Nell, J. (2003). An assessment of alternative processes for the production of  $TiO_2$  pigments by chlorination. Chem. Technol., **27** (September), 29–30.
2. Luckos, A. and Den Hoed, P. (2004). Fluidization and flow regimes of titaniferous solids. Ind. Eng. Chem. Res., **43**, 5645–5652.
3. Luckos, A. and Den Hoed, P. (2005a). Pressure and solid distributions in the riser of a circulating fluidized bed. In Cen, K. (ed.) Circulating Fluidized Bed Technology VIII, 231–238. Beijing: International Academic Publishers/Beijing World Publishing Corporation.
4. Luckos, A. and Den Hoed, P. (2005b). A study into the hydrodynamic behaviour of heavy minerals in a circulating fluidized bed. In Luckos, A. & Smit, P. (eds) IFSA 2005, Industrial Fluidization South Africa, 345–355. Johannesburg: SAIMM.
5. Lackermeier, U. and Werther, J. (2002). Flow phenomena in the exit zone of a circulating fluidized bed. Chem. Eng. Process., **41**, 771–783.



6. Brereton, C.M.H. and Grace, J.R. (1993). End effects in circulating fluidized bed hydrodynamics. *In* Avidan, A.A. (ed.) Circulating Fluidized Bed Technology IV, 137–144. New York: AIChE.
7. Zheng, Q.-Y. and Zhang, H. (1995). Effect of geometry of bed exit (end effect) on hydrodynamic behaviour of gas-solid flow in CFB combustor. Fluidization VIII, Preprint, Volume 2, 657–664. Toulouse, France: Progep.
8. Pugsley, T., LaPointe, D., Hirschberg, B. and Werther, J. (1997). Exit effects in circulating fluidized bed risers. Can. J. Chem. Eng., **75**, 1001–1010.
9. Jin, Y., Yu, Z., Qi, C. and Bai, D.-R. (1988). The influence of exit structures on the axial distribution of voidage in fast fluidized bed. *In* Kwauk, M. and Kunii, D. (eds) Fluidization '88 Science and Technology, 165–173. Beijing: Science Press.
10. Johnsson, F., Zijerveld, R.C., Schouten, J.C., Van den Bleek, C.M. and Leckner, B. (2000). Characterization of fluidization regimes by time-series analysis of pressure fluctuations. Int. J. Multiphase Flow, **26**, 663–715.
11. Xu, J., Bao, X., Wei, W., Shi, G., Shen, S., Bi, H.T., Grace, J.R. and Lim, C.J. (2004). Statistical and frequency analysis of pressure fluctuations in spouted beds. Powder Technol., **140**, 141–154.
12. Du, B., Warsito, W. and Fan, L.-S. (2006). Behavior of the dense-phase transportation regime in a circulating fluidized bed. Ind. Eng. Chem. Res., **45**, 3741–3751.
13. Press, W.H., Teukolsky, S.A., Vetterling, W.T. and Flannery, B.P. (1994). Numerical Recipes in FORTRAN: The Art of Scientific Computing. 2nd edition. Cambridge: Cambridge University Press.
14. Zijerveld, R.C., Johnsson, F., Marzocchella, A., Schouten, J.C. and Van den Bleek, C.M. (1998). Fluidization regimes and transitions from fixed bed to dilute transport flow. Powder Technol., **95**, 185–204.
15. Bai, D., Shibuya, E., Nakagawa, N. and Kato, K. (1996). Characterization of gas fluidization regimes using pressure fluctuations. Powder Technol., **87**, 105–111.
16. Chang, H. and Louge, M. (1992). Fluid dynamic similarity of circulating fluidized beds. Powder Technol., **70**, 259–270.
17. Glicksman, L.R., Hyre, M.R. and Woloshun, K. (1993). Simplified scaling relationships for fluidized beds. Powder Technol., **77**, 177–199.
18. R.C. Brown, R.C. and E. Brue, E. (2001). Resolving dynamical features of fluidized beds from pressure fluctuations. Powder Technol. **119**, 68–80.
19. Van der Stappen, M.L.M., Schouten, J.C. and Van den Bleek, C.M. (1993). Application of deterministic chaos analysis to pressure fluctuations measurements in a 0.96 m<sup>2</sup> CFB riser. *In* Avidan, A.A. (ed.) Circulating Fluidized Bed Technology IV, 54–61. New York: AIChE.
20. Van der Schaaf, J., Johnsson, F., Schouten, J.C. and Van den Bleek, C.M. (1999). Fourier analysis of nonlinear pressure fluctuations in gas-solids flow in CFB risers—Observing solids structures and gas/particle turbulence. Chem. Eng. Sci., **54**, 5541–5546.
21. Johnsson, F., Larson, G. and Leckner, B. (2002). Pressure and flow fluctuations in a fluidized bed—Interaction with the air-feed system. Chem. Eng. Sci., **57**, 1379–1392.